

Parallel Fourier domain optical coherence tomography for in vivo measurement of the human eye

Branislav Grajciar^{1,3}, Michael Pircher¹, Adolf F. Fercher¹, Rainer A. Leitgeb^{1,2}

¹Centre of Biomedical Engineering and Physics, Medical University of Vienna, Waehringer Str. 13, A-1090 Vienna, Austria

²Laboratoire d'Optique Biomedicale, Ecole Polytechnique Fédéral de Lausanne, CH-1015 Lausanne, Suisse

³Department of Radioelectronics, Slovak University of Technology FEEIT, SK-81219 Bratislava, Slovak Republic
rainer.leitgeb@meduniwien.ac.at

Abstract: A parallel Frequency Domain Optical Coherence Tomography (FD-OCT) system and - to the best of our knowledge- first in vivo tomograms obtained with such system are presented. A full tomogram of 256(x) x 512(z) pixels covering a sample region of 8 mm x 3,8 mm is recorded in only 1 ms. Since the transverse as well as the depth information is obtained in parallel, the structure is free of any motion artifacts. In order to study cross talk issues for parallel illumination the transversal resolution for a thermal light source is compared to that with an SLD.

©2005 Optical Society of America

OCIS codes: (170.4500) Medical optics and biotechnology: Optical coherence tomography, (170.4460) Medical optics and biotechnology: Ophthalmic optics

References and links:

1. A. F. Fercher, C. K. Hitzenberger, G. Kamp, and S. Y. El-Zaiat, "Measurement of intraocular distances by backscattering spectral interferometry," *Opt. Commun.* **117**, 43-48 (1995).
2. R. A. Leitgeb, C. K. Hitzenberger, and A. F. Fercher, "Performance of Fourier domain vs. time domain optical coherence tomography," *Opt. Express* **11**, 889-894 (2003).
<http://www.opticsexpress.org/abstract.cfm?URI=OPEX-11-8-889>
3. J. F. de Boer, B. Cense, B. Hyle Park, M. C. Pierce, G. J. Tearney, B. E. Bouma, "Improved signal-to-noise ratio in spectral-domain compared with time-domain optical coherence tomography," *Opt. Lett.* **28**, 2067-2069 (2003).
4. M. Wojtkowski, T. Bajraszewski, P. Targowski, A. Kowalczyk, "Real-time in vivo imaging by high-speed spectral optical coherence tomography," *Opt. Lett.* **28**, 1745-1747 (2003).
5. R. A. Leitgeb, L. Schmetterer, W. Drexler, A. F. Fercher, R. J. Zawadzki, and T. Bajraszewski, "Real-time assessment of retinal blood flow with ultrafast acquisition by color Doppler Fourier domain optical coherence tomography," *Opt. Express* **11**, 3116-3121 (2003).
<http://www.opticsexpress.org/abstract.cfm?URI=OPEX-11-23-3116>
6. N. Nassif, B. Cense, B. H. Park, S. H. Yun, T. C. Chen, B. E. Bouma, G. J. Tearney, and J. F. de Boer, "In vivo human retinal imaging by ultrahigh-speed spectral domain optical coherence tomography," *Opt. Express* **29**, 480-482 (2004).
<http://www.opticsexpress.org/abstract.cfm?URI=OPEX-12-3-367>
7. S. H. Yun, G. J. Tearney, J. F. de Boer, B. E. Bouma, "Motion artifacts in optical coherence tomography with frequency-domain ranging," *Opt. Express* **12**, 2977-2998 (2004).
<http://www.opticsinfobase.org/abstract.cfm?id=80320>
8. M. Laubscher, M. Ducros, B. Karamata, T. Lasser, R., Salathe "Video-rate three-dimensional optical coherence tomography," *Opt. Express* **10**, 429-435 (2002).
<http://www.opticsexpress.org/abstract.cfm?URI=OPEX-10-9-429>
9. E. Beaurepaire, A. C. Boccara, M. Lebec, L. Blanchot, H. Saint-Jalmes, "Full-field optical coherence microscopy," *Opt. Lett.* **23**, 244-246 (1998).
10. A. F. Zuluaga, R. Richards-Kortum, "Spatially resolved spectral interferometry for determination of subsurface structure," *Opt. Lett.* **24**, 519-521 (1999).
11. R. J. Zawadzki, C. Leisser, R. Leitgeb, M. Pircher, A. F. Fercher, "Three-dimensional ophthalmic optical coherence tomography with a refraction correction algorithm," *SPIE Proc.* **5140**, 20-27 (2003).

12. V. Westphal, A. M. Rollins, S. Radhakrishnan, J. A. Izatt, "Correction of geometric and refractive image distortions in optical coherence tomography applying Fermat's principle," *Opt. Express* **10**, 397-404 (2002).
<http://www.opticsinfobase.org/abstract.cfm?id=68842>.
13. R. A. Leitgeb, W. Drexler, A. Unterhuber, B. Hermann, T. Bajraszewski, T. Le, A. Stingl, A. F. Fercher "Ultra-high resolution Fourier domain optical coherence tomography," *Opt. Express* **12**, 2156-2165 (2004).
<http://www.opticsexpress.org/abstract.cfm?URI=OPEX-12-10-2156>.
14. A. F. Fercher, C. K. Hitzenberger, M. Sticker, R. Leitgeb, E. Barriouso "A thermal light source technique for optical coherence tomography," *Opt. Commun.* **185**, 57-64 (2000).
15. B. Karamata, P. Lambelet, M. Laubscher, R. P. Salathé, T. Lasser, "Spatially incoherent illumination as a mechanism for cross-talk suppression in wide-field optical coherence tomography," *Opt. Lett.* **29**, 736-738 (2004).
16. R. Henderson, K. Schulmeister, *Laser Safety* (Institute of Physics Publishing, London 2004).
17. American National Standards Institute, *Safe Use of Lasers, ANSI Z136.1-2000*, (Laser Institute of America, 2000).
18. A. F. Fercher, R. Leitgeb, C. K. Hitzenberger, H. Sattmann, M. Wojtkowski, "Complex Spectral Interferometry OCT," *Proc. SPIE* **3564**, 173-178 (1998).
19. M. Wojtkowski, A. Kowalczyk, R. Leitgeb, A. F. Fercher, "Full range complex spectral optical coherence tomography technique in eye imaging," *Opt. Lett.* **27**, 1415-1417 (2002).
20. R. A. Leitgeb, C. K. Hitzenberger, T. Bajraszewski, A. F. Fercher, "Phase Shifting Algorithm to achieve high speed long depth range probing by Fourier Domain Optical Coherence Tomography," *Opt. Lett.* **28**, 2201-2203 (2003).

1. Introduction

Recent works on Fourier Domain Optical Coherence Tomography (FD OCT) - first introduced to the field of biomedical imaging by Fercher et al. in 1995 [1] - demonstrated the impressive potential of this technique to perform fast in-vivo imaging of biological tissue with high sensitivity as well as high resolution. The speed advantage as compared to time domain OCT systems is based on the fact, that the full depth structure is recorded in parallel without need of depth scanning. The imaging speed could thereby be improved by a factor of 40 and more, up to an A-line rate of 30 kHz [2-6]. Still one needs to perform lateral scanning of the sample that ultimately limits the imaging speed. Especially in applications where an exact knowledge of the structure is necessary any movements during the lateral scanning cause structural deformations in the tomograms. The measurement time should therefore be extremely short in order to minimize such movement artifacts [7]. Parallel time domain OCT was a first step to avoid the lateral scanning by recording the full transversal object structure synchronously with a smart pixel detection array [8]; still, the necessary depth scanning limited the achievable tomogram rate. The same applies to full field optical coherence microscopy [9], where in addition a phase shifting device is needed. In 1999 Zuluaga and Richards-Kortum [10] reported a fully parallel FD OCT system that needs neither lateral nor longitudinal scanning. They imaged a fixed technical sample for demonstrating the principle. The content of the current work is to present a fully parallel FD OCT system that allows *in-vivo* real time imaging of human eye structures. The motivation is to use the measured data as input to ray tracing routines that allow a true geometrical reconstruction of eye interfaces and their topology [11].

2. Methods

2.1 Experimental setup

Figure 1(a) shows a scheme of the setup. In order to produce a slit illumination on the sample the collimated light is passed through a cylindrical lens CL ($f=100$ mm). A chopper wheel is placed in the focal plane of the lens. It is needed for blocking the light during the read out process of the CCD camera. The slit dimension on the sample after lenses L2 and L3 (achromat, $f=100$ mm) is $8.6 \mu\text{m} \times 12$ mm. (Fig. 1(b)).

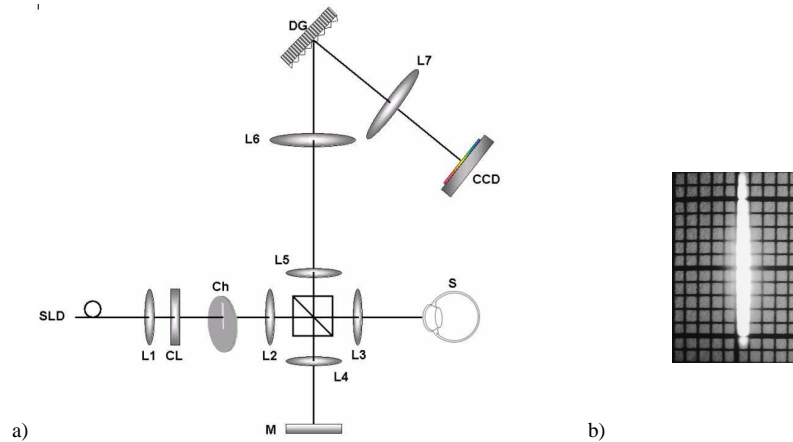


Fig. 1. (a) The schematic of the Parallel FD OCT system. SLD - light source; L1 – collimator; CL-cylindrical lens, $f=100$ mm; L1- L5 - achromatic lens $f=100$ mm; NPBS - non-polarizing beam splitter 50:50; L6, L7 - achromatic lens $f=310$ mm; DG – diffraction grating; (b) Demonstration of line illumination (millimeter scale)

Two different light sources were used for illumination: a SLD (Superlum Diodes Ltd) with the central wavelength at 811 nm and a full width at half maximum spectral width (FWHM) of 17 nm, and a halogen lamp with a center wavelength of 800 nm and an optically filtered FWHM of 100 nm. Figure 2 displays both spectra together with the temporal coherence functions of the light exiting from the interferometer. For the SLD one achieves a theoretical axial resolution of $17 \mu\text{m}$ whereas for the halogen lamp the axial resolution is $3 \mu\text{m}$ (Fig. 2(b)). The power at the sample for the SLD was 2 mW, whereas for the halogen lamp it was only $500 \mu\text{W}$.

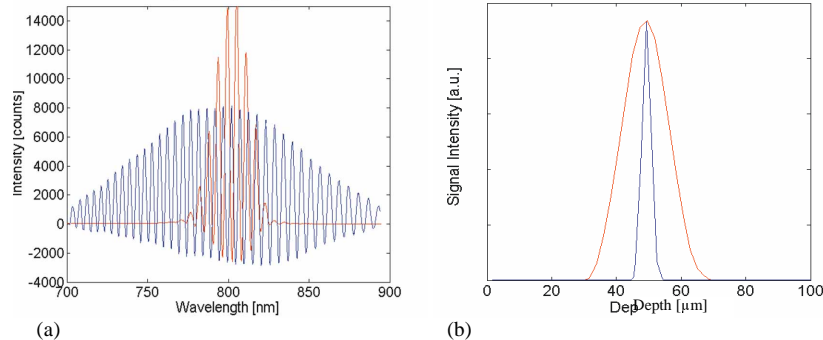


Fig. 2. (a) Spectrum of the interferometer output after subtraction of the reference arm light: SLD (Red), Halogen Lamp (Blue), (b) Normalized coherence envelope after FFT of (a): SLD (Red), Halogen Lamp (Blue).

An anamorphic optical scheme is used. The beam propagation and optical arrangement for the vertical and horizontal planes of that scheme are shown in Fig. 3. The point spread function in the camera plane after the camera lens (achromatic doublet $f=310$ mm) has a $1/e^2$ diameter of $8.6 \mu\text{m}$ with a beam waist of 12 mm at lens L7. With a CCD pixel size of $26 \mu\text{m} \times 26 \mu\text{m}$ diffraction limited detection is assured. The line illumination can be viewed as a set of parallel channels, each of them associated with a different transverse position on the sample. These channels are spectrally dispersed by the diffraction grating (1800 lines/mm for the SLD and 1200 lines/mm for the thermal light) and recorded individually on different vertical lines of the CCD area (Andor H1024 x V256, 1 MHz ADC). The transversal field of view captured

by the camera finally amounts to 6.7mm. One full tomogram of 256(x) x 512(z) pixels is recorded in only 1ms. The data readout and post processing need in total 300 ms. Hence with the current equipment a full tomogram repetition rate of 3 Hz is achieved. This is mainly limited by the digital-to-analog conversion speed of the CCD. There are already commercially available CCD systems that would allow for 60 tomograms per second and more.

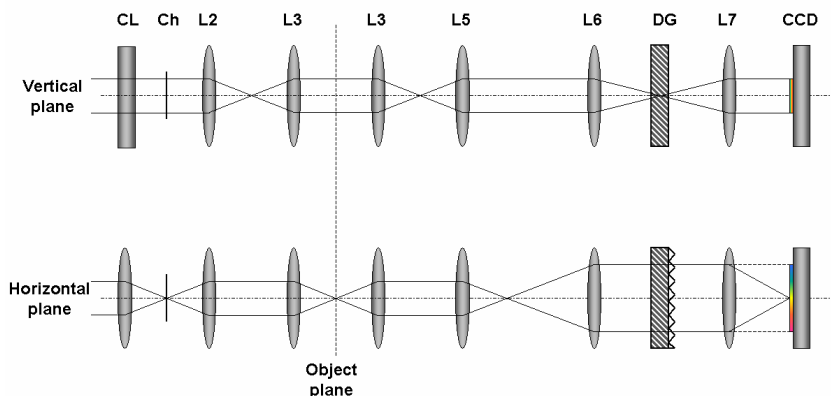


Fig. 3. Diagrams of optical paths for two orthogonal planes of the anamorphic optical system. The abbreviations are the same as in Fig. 1.

2. 2 Sensitivity and resolution

As already mentioned the important advantage of FD OCT system in comparison to TD OCT setups is the increased sensitivity [2, 3]. Since the power is distributed over all parallel channels one ends up with a factor of 1/100 or less of the illumination power for each transverse channel. The SLD allowed for an optical power of $8 \mu\text{W}$ per transversal channel (2mW divided by the 250 lines of the CCD). A theoretical analysis shows that with a mere power of $8 \mu\text{W}$ it is still possible to achieve a shot noise limited sensitivity of 96 dB for an exposure time of 1 ms with FD OCT [2, 3]. The experimental sensitivity of our system in the center of the transverse slit is 89 dB. It was measured with an attenuation of -40 dB in the sample arm and by adjusting the reference arm power until the recorded spectrum was close to the saturation level of the CCD. The sensitivity was then calculated by measuring the signal-to-noise ratio (SNR) between signal peak after FFT and the ambient noise rms and accounting for the additional -40 dB attenuation. Ideally the exposure time should be reduced to < 1 ms to avoid blurring and averaging of the interference fringes on the CCD [2, 7]. An increased background level due to coherent and incoherent cross talk might cause the difference of the measured sensitivity to the theoretical value. It was shown recently that an increase of incoherent background has a strong adverse effect on the system sensitivity and dynamic range [13]. Moreover, only 7 mm of the full 12 mm line are actually imaged onto the CCD, which additionally decreases the effective system sensitivity.

The lateral resolution of the system can be measured by determining the smallest resolvable element of a USAF chromium resolution test target (RTT) (USAF 1951 chromium positive 04TRP003, Melles Griot) that is clearly resolved (peak maximum is bigger than twice the modulation depth, disregarding the background). Two types of light sources, an SLD and a thermal Tungsten Halogen Lamp, are compared to see how their spatial coherence properties affect the transverse resolution. The smallest resolvable elements for SLD and halogen lamp were 6.35-line pairs/mm (group 2 element 5) and 11.3-line pairs/mm (group 3 element 4) respectively (Fig. 4). This corresponds to a lateral resolution of $\sim 100 \mu\text{m}$ and $\sim 50 \mu\text{m}$ respectively. The chosen optics (Fig. 1) allows for a one-to-one imaging relation between the transverse extension of the probed sample region and the vertical CCD plane size. Hence the theoretical maximal resolution is given according to the sampling theorem by twice the pixel size of the CCD, i.e. $50 \mu\text{m}$. One observes that the lateral resolution with the thermal light

source matches the theoretical limit, whereas for the SLD it is almost two times worse. This can be attributed to coherent cross talk in case of the SLD. A spatially incoherent light source on the other hand can be viewed of as a set of parallel channels, which consists of a multitude of spatially coherent image spots. The extension of these spots is given by Van Zitter - Zernike's theorem [14]. Since there is no statistic correlation between different spots it can be clearly seen that the spatial incoherence of thermal light provides an efficient mechanism for suppression of coherent crosstalk [15].

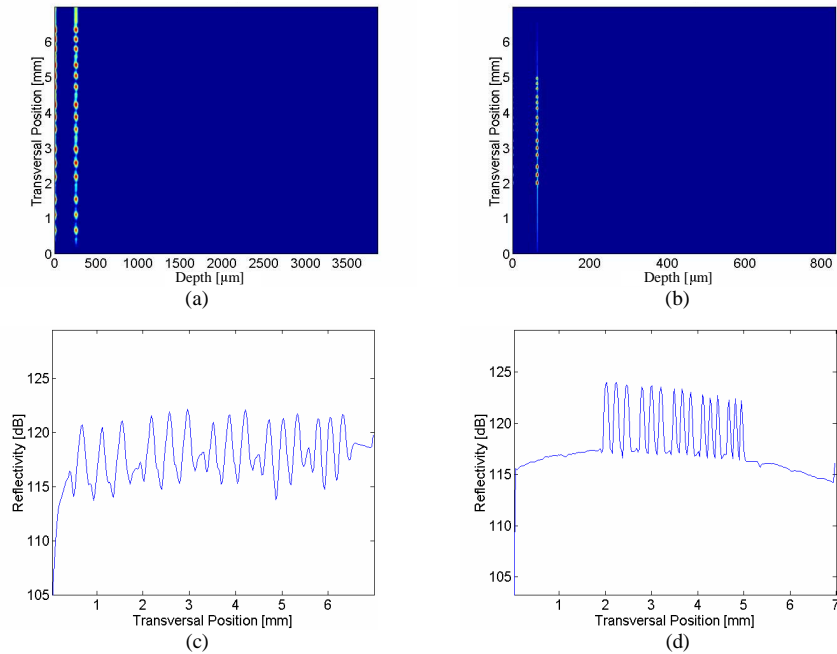


Fig. 4. (a) OCT tomogram of RTT- Group 1 – with SLD; (b) OCT tomogram of RTT- Group 2 with Halogen Lamp; (c) Cross section along the RTT surface for SLD, and in (d) for the Halogen Lamp.

Nevertheless the power of the thermal light source was too small for an efficient imaging of biological tissue. Moreover the broad spectrum allows only for a limited depth range. For these reasons, the SLD was chosen for the subsequent in-vivo experiments.

2.3. Laser safety issues

Since the beam at the sample forms a line one has different illumination properties of the horizontal and vertical incident planes. The beam has a high divergence after the eye lens in the meridional plane, and is focused onto the retina in the saggital direction [16]. According to the ANSI standards [17] of laser safety the retinal thermal exposure limits depend on the angular subtense α of the apparent source. Since the lenses L2 and L3 form a telescope with enlargement equal to one, the position of cylindrical lens relative to the eye is virtually the same as that of lens L3. The angular subtense depends on the position of the eye relative to the focal plane of lens L3. In the present case the focal plane lies somewhere between the cornea and the eye lens, i.e., $\alpha = 12 \text{ mm}/100 \text{ mm} = 120 \text{ mrad}$ (Fig. 5). Assuming an eye exposure time of $t=100 \text{ s}$, one obtains for the maximal permissible exposure at $\lambda = 811 \text{ nm}$, $\text{MPE} = 9.12 \text{ mW} \cdot \text{mm}^{-2}$.

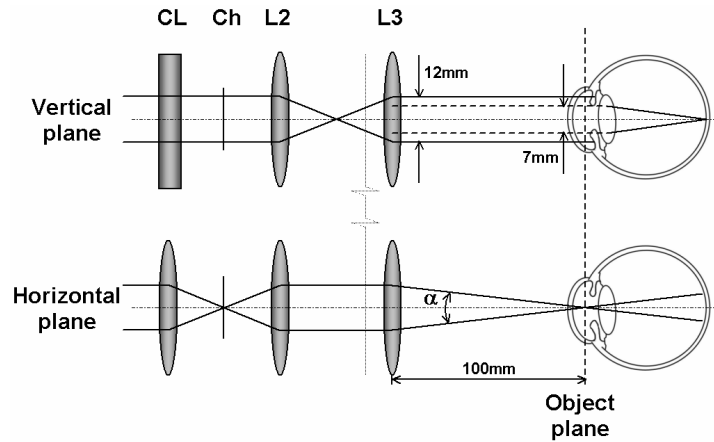


Fig. 5. Calculation of MPE for the eye

One can see that an illumination of 2 mW along a line of 12 mm is well below the MPE for eye exposure. Nevertheless, one should take into account that the power distribution along the line is not homogeneous but follows a Gaussian profile. This effect is minimized by choosing a line height at the sample of 12 mm that is larger than the actual eye pupil diameter of ~ 7 mm.

3. Results and discussion

Figure 6(a) and (b) show the angular region of the anterior chamber of a healthy volunteer. It is a well-known fact that FDOCT suffers from a decrease of SNR with increasing depth range. In the present case a SNR drop of 14 dB as one advances to the maximal depth position was measured. This decay follows a *sinc* function and is determined by the horizontal pixel width of the CCD [2]. In order to compensate for this effect, each depth profile was corrected by multiplication with a function that shows the inverse behavior of the decay. This method is basically a deconvolution technique. Figure 6(a) and (b) show images of the chamber angle before and after the correction. One observes an increased contrast especially in the iris region. Figure 6(c) shows a tomogram of the full anterior chamber.

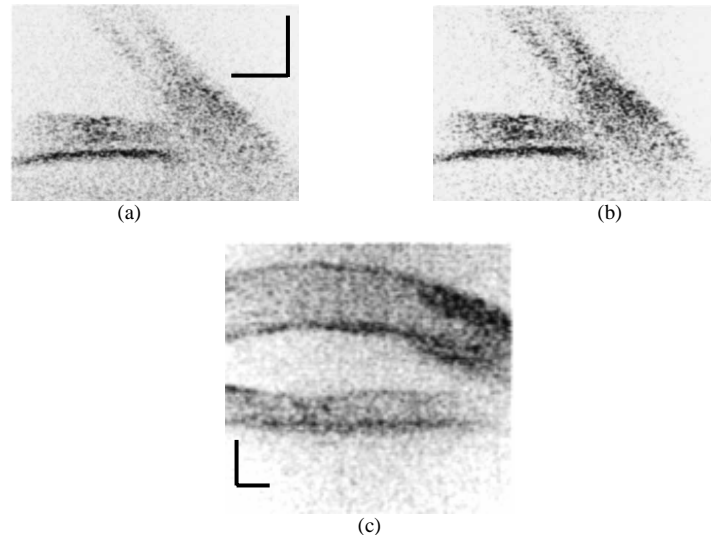


Fig. 6. Human eye *in vivo* - Anterior chamber angle (a) without and (b) with correction. (c) Cornea and iris at a position close to iris rim; the scale bars correspond to 1mm vertically and 0.5mm horizontally.

The current achievable depth range is not sufficient for imaging the central part of the cornea together with the iris; therefore a region close to the rim of the iris was chosen. At this position the iris appears fully closed. However, the depth range limitation can be relaxed by using phase shifting algorithms [18, 19, 20].

4. Conclusions

In conclusion a parallel FD OCT system is presented that is capable of imaging biological structures *in vivo*. To the best of our knowledge the first *in vivo* tomograms obtained with a full parallel FD OCT system are presented. The system shows sufficient sensitivity to image biological tissue despite the small power of 8 μW for each transversal channel. A full tomogram is recorded in only 1ms. Being free of any motion artifacts this data is of great value for investigating the optical properties such as topography and refractive power of the cornea and lens of the human eye. It is demonstrated that a spatially incoherent light source such as the halogen lamp allows for an efficient suppression of coherent crosstalk resulting in an increased transversal resolution. Although such light source would be the ideal choice for a parallel detection system the small available output power limits its use for fast imaging of biological samples.

Acknowledgments

Carl Zeiss Meditec Inc. is acknowledged for providing a PhD scholarship and inventory. The Austrian Fonds zur Förderung der wissenschaftlichen Forschung (FWF grant P16776-N02) is acknowledged for financial support.